Journal of Physics: Conference Series **2391** (2022) 012007 doi:10.1088/1742-6596/2391/1/012007

A new light particle is being born

A.J. Krasznahorkay[1], M. Begala[1,3], M. Csatlós[1], L. Csige[1], J. Gulyás[1], A. Krakó[1,3], A. Krasznahorkay[1] [1], B.M. Nyakó[1], I. Rajta[1], N.J. Sas[1,3], J. Timár[1], I. Vajda[1]

[1]Institute for Nuclear Research (ATOMKI), H-4001 Debrecen, P.O. Box 51
[3]University of Debrecen, 4010 Debrecen, PO Box 105, Hungary

E-mail: `kraszna@atomki.hu`

Abstract.
A few years ago we observed anomalous electron-positron angular correlations for the 18.15 MeV M1 transition of ^{8}Be. This was interpreted as the creation and decay of an intermediate bosonic particle with a mass of m_0c^2=16.70±0.35(stat)±0.5(sys) MeV, which is now called X17. The possible relation of the X17 boson to the dark matter problem triggered an enormous interest in the wider physics community. We also observed a similar anomaly in ^{4}He, which could be described also by the creation and subsequent decay of the same X17 particle. Very recently, the ^{11}B proton capture reaction was used for exciting the 17.2 MeV broad (Γ= 1.15 MeV) resonance in ^{12}C and studying their internal pair creation decay. Anomalies were observed in the angular correlation of the electron-positron pairs, which together with the ^{8}Be and ^{4}He data provides kinematic evidence for the X17 particle and supports their vector boson and fifth force explanation.

1. Introduction

Our current knowledge of nature at the fundamental level is successfully explained by the Standard Model (SM) of elementary particles, but this theory describes only five percent of the entire content of the Universe. We named the overwhelming unknown constituents as dark matter and dark energy. The nature of dark matter is currently one of the greatest unsolved mysteries in physics.

The search for new physics beyond the SM can be divided into two categories. The first one is the search for new heavy particles and interactions at high energies, the so-called "energy frontier" research. A complementary and vital role is played by low-energy, precision and/or high-intensity experiments, which require a joint effort of the particle, atomic, and nuclear physics communities [1, 2]. One of the main targets of the intensity frontier in particle physics is a new force carrier which is much lighter than the weak scale and which interacts with the Standard Model particles very weakly. Observations of rare nuclear transitions can be used to search for new hidden force-carrier particles at the MeV scale. In this approach, a fixed target is bombarded with a hadron beam to produce excited states of a nucleus. The excited state then also decays by emitting new particles.

Recently, we have observed an anomaly in the nuclear decay of ^{8}Be [3]. The ^{7}Li(p,γ)^{8}Be reaction was used to populate the excited states in ^{8}Be selectively and the differential internal

[1] Present address: CERN, Geneva, Switzerland

pair conversion coefficients were studied for the 17.6 MeV, and 18.15 MeV ($J^\pi = 1^+ \rightarrow 0^+$) M1 transitions in ^{8}Be. Significant, peak-like enhancement of the internal pair creation [4] was observed at large angles in the angular correlation of the 18.15 MeV transition, but not in the 17.6 MeV one [3]. This observation was interpreted as the creation and the subsequent decay of an X boson with mass m_0c^2=16.70±0.35(stat)±0.5(sys) MeV. The branching ratio of the e^+e^- decay of such a boson to the γ decay of the 18.15 MeV level of ^{8}Be is found to be 5.8×10^{-6} [3].

J. Feng and his group [5, 6] studied our data along with other previous experiments and showed that our observation strongly disfavors dark photons. Instead, they proposed a new theory and explained the observation by introducing a fifth fundamental force [5]. If confirmed by further experiments, this discovery of a possible fifth force would completely change our understanding of the universe, by taking a step towards the unification of forces and dark matter.

The possible relation of the X boson to the dark matter problem and the fact that it might explain the $(g\text{-}2)_\mu$ puzzle triggered an enhanced theoretical and experimental interest in the particle and hadron physics community [7]. Inspired by this enhanced interest, we studied the effect in other nuclear reactions using improved experimental conditions.

2. Measurement of e$^+$e$^-$ angular correlation

The high-lying energy levels of ^{8}Be were excited by proton radiative capture on ^{7}Li target. The protons were produced using a home-built Van de Graaff accelerator at ATOMKI. In order to measure the angular correlation of the e$^+$e$^-$ pairs, we have built a highly efficient spectrometer with high angular resolution that no one has used before [8]. We are talking about observing a very rare process, the probability of which is one million times (10^{-6}) lower compared to the probability of electromagnetic transition (γ-radiation). The detection of the new particle is further complicated by the fact that in high-energy electromagnetic transitions, according to quantum electrodynamics, e$^+$e$^-$ pairs can also be created. These provide a significant background for our measurements, since the probability of the process called Internal Pair Creation (IPC) is about one thousandth (10^{-3}) of the probability of a γ-transition. However, the angular correlation between the resulting e$^+$e$^-$ pairs is well known, and with good approximation the IPC rate decreases exponentially depending on the angle between the two particles, and to contrast that to the sharp peak around a non-rero opening angle for the decay of a massive particle. Detecting these very rare events was a significant challenge for our e$^+$e$^-$ coincidence spectrometer. The spectrometer consists of 5 Multiwire Proportional Counters (MWPC) and thin (ΔE) and thick (E) plastic scintillation detectors. The schematic diagram of the spectrometer can be seen in Figure 1.

The detectors of the spectrometer were sufficiently stable during the typically 1-week experiments, we only saw changes in the gain of a few % in the scintillation detectors, which were corrected during the data analysis. The efficiency (acceptance) of the spectrometer was determined experimentally, depending on the correlation angle, using uncorrelated e$^+$e$^-$ events collected simultaneously with e$^+$e$^-$ coincidence events. With this efficiency, we corrected the angular correlation of all internal pairs coming from the target. In Figure 2(a), the energy-sum spectrum of e$^+$e$^-$ pairs measured after the decay of the 17.6 MeV excited state of ^{8}Be is presented.

This state was excited by resonant proton capture. The energy of the resonance is E_p= 441 keV, and the width is Γ=10.7 keV. The 17.6 MeV transition in the spectrum goes to the ground state of ^{8}Be, while the 14.6 MeV goes to the very broad first excited state, decaying to two α-particles. The intense ^{16}O line at the beginning of the spectrum is excited by the ^{19}F(p,α)^{16}O reaction in the LiF target used in this case. In Figure 2(b) the angular correlation of the 17.6 MeV and 14.6 MeV transitions are indicated. The full curves marked with M1 and E1 are the result of simulations assuming magnetic and electrical dipole transitions.

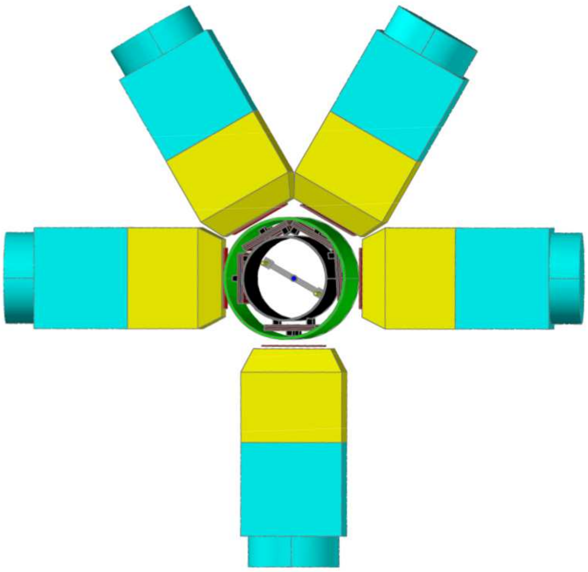

Figure 1. Schematic diagram of the electron-positron pair spectrometer.

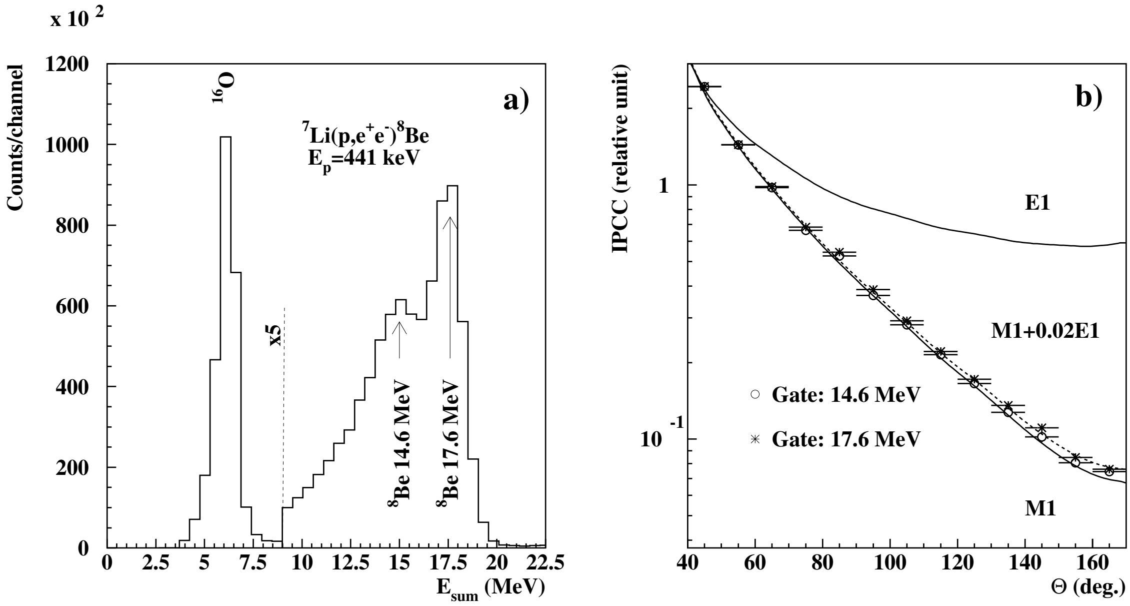

Figure 2. Measured total energy spectrum (a) and angular correlation (b) of the e^+e^- pairs originated from the decay of the 17.6 MeV resonance compared with the simulated angular correlations assuming M1 (full curve) and M1+1.4%E1 mixed transitions (dashed line).

Monte Carlo simulations for the experiment were conducted with the GEANT [9] code developed at CERN. Every part of the spectrometer, to the last screw in the vicinity of the target, is carefully incorporated into the simulation to obtain the spectrometer's response to both e^+e^- pairs and intense γ radiation. In addition to the internal pair creation process, we also took into account the background caused by γ radiations, external pair creation and e^- and

e^+ multiple scattering in order to understand as accurately as possible the response functions of the detectors and spectrometers.

As shown in Figure 2, in line with previous results, above 110° we have observed a slight difference between the experimental values and the values simulated for the M1 transition. As far as we know, this transition should be a clean M1 transition. However, if we also take into account the effect of the weak, non-resonant E1 multipolarity background generated by direct proton capture by mixing only 1.4% E1 angular correlation to the M1 angular correlation, then we can already interpret our experimental results accurately. The degree of continuous background mixing to the resonance depends on both the width of the resonance and the thickness of the target, which causes the broadening of the resonance.

After this experiment, we also examined the angular correlation of e^+e^- pairs from a higher excited state of 18.15 MeV, which was also well known. Our experimental angular correlations measured on the E*= 18.15 MeV resonance can be seen in Figure 3.

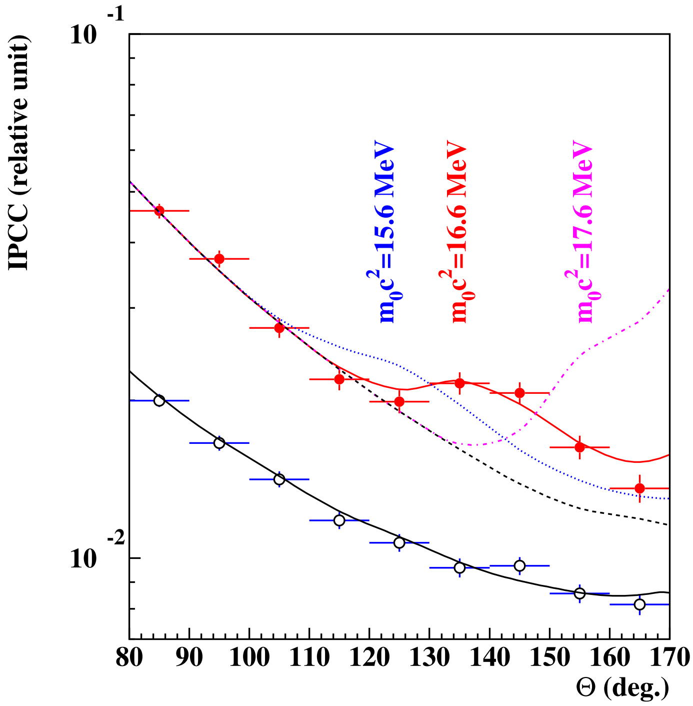

Figure 3. Experimental angular e^+e^- pair correlations measured in the ^{7}Li(p,e^+e^-)^{8}Be reaction at E_p=1.10 MeV with -0.5 ≤ y ≤ 0.5 (full circles) and $|y|$ ≥ 0.5 (open circles) (see the definition of y in the text). The results of simulations of boson decay pairs added to those of IPC pairs are shown for different boson masses, with different colors.

This state can also be excited resonantly, with protons of 1.040 MeV, but the resonance is much wider (Γ=138 keV) than the previous resonance. Therefore, a much larger mixing can be expected from the non-resonant E1 background. This was confirmed by previous experimental results published for the range of 75° to 130° [10].

In this experiment, we extended our angular range up to 170°, and as a result of the ≈3 orders of magnitude larger efficiency compared to the spectrometer built by Stiebing et al.[10], we also significantly reduced the statistical error of measurement.

It is important to note that the distributions were collected for e^+e^- pairs with a near symmetrical energy distribution:

$$-0.5 < \frac{E_{e^-} - E_{e^+}}{E_{e^-} + E_{e^+}} < 0.5 \; , \tag{1}$$

where E_{e^-} represents the energy of the electron, while E_{e^+} represents the energy of the positron. To the best of our knowledge, the significant anomaly observed at 140° cannot currently be explained reliably by a nuclear physics effect. The difference between the experimental and theoretical values is significant and can be explained by the introduction of a new particle (X17) with a mass of 16.7±0.35 (statistical error) ±0.5 (systematic error) MeV. The probability of formation of e^+e^- pairs when the particle decayed was 5.8×10^{-6} compared to the probability of a γ transition (branching ratio).

Assuming X17, the different theoretical descriptions give different values for the X17 branching ratios of the 17.6 MeV excited state as well [5, 6, 11, 12]. This should be further investigated both experimentally and theoretically.

3. Experiments with the new Tandetron accelerator

3.1. Study of the e^+e^- angular correlation from the $^3H(p,e^+e^-)^4He$ reaction [13]

The e^+e^- angular correlation was studied from the above reaction at E_p = 510, 610 and 900 keV proton energies to search for signatures of the X17 particle. This reaction induced direct capture [14] and resonant capture and populate the overlapping $J^\pi = 0^+$ first, and $J^\pi = 0^-$ second excited states in ^{4}He [15].

The proton beam with a typical current of 1.0 μA was impinged on a ^{3}H target for about 100 hours for each bombarding energy. The ^{3}H was absorbed in a 4.2 mg/cm^2 thick Ti layer evaporated onto an 0.4 mm thick molybdenum disk with a diameter of 50 mm. The density of the ^{3}H atoms was $\approx 2.7\times10^{20}$ atoms/cm^2. The disk was cooled down to liquid N_2 temperature to prevent ^{3}H evaporation. In such a thick ^{3}H+Ti target, the proton beam was stopped completely. The target was shifted off the center of the spectrometer by 25 mm downstream along the proton beam axis to avoid the screening by the target backing and holder. We have used a large (50 mm diameter) cooling pipe with a fixing screw, which limited the maximal correlation angle to ≈ 140°, since the surface of the target was inside the pipe.

The proton energies were chosen to stay below the threshold of the (p,n) reaction (E_{thr}=1.018 MeV). The ^{4}He nucleus was excited up to E_x = 20.21, 20.29 and 20.49 MeV at the used proton beam energies, so it was expected that the first excited state of ^{4}He (J^p=0^+, E_x=20.21 MeV, Γ=0.50 MeV) and the second one (J^p=0^-, E_x=21.01 MeV, Γ=0.84 MeV) were both populated [15].

Our previous experimental setup [3, 8] has recently been upgraded by the replacement of the scintillators with EJ200 ones and PM tubes by Hamamatsu 10233-100 ones. The sizes of the scintillators were $82\times86\times80$ mm^3 each.

As another improvement, the Multi Wire Proportional Chambers (MWPC) have been replaced by novel Double-sided Silicon Strip Detectors (DSSD), placed very close to the front face of the scintillators, to enhance the efficiency of the experimental setup and its homogeneity.

We also increased the number of telescopes from 5 to 6. The positions of the hits were registered by the DSSDs having sizes of 50×50 mm^2, strip widths of 3 mm and a thickness of 500 μm. The telescope detectors were perpendicular to the beam direction, each at 60° to its neighbors, around a vacuum chamber made of a carbon fiber tube with a wall thickness of 1 mm.

3.2. Validating the results of the simulations

In order to test the accuracy of the GEANT simulations for describing our experiments, we made measurements with the previously described ^{7}Li(p,γ)^{8}Be reaction.

A ^{7}Li target was evaporated onto the same Ti+Mo backing that the ^{3}H target used, in the same geometrical setup as described earlier. Since the internal pair creation coefficient calculated by Viviani et al. [16] for ^{4}He is only slightly higher than that calculated one for the 17.6 MeV transition in ^{8}Be, this transition allowed us to accurately test the backgrounds coming from γ radiation in our main experimental setup as well.

The ratio of the event numbers used for the simulations are determined by the internal pair creation coefficient as described before. These IPC+EPC simulations provided an accurate description of the experimental data. The contribution of the IPC and EPC processes to the events selected by our analysis in this case is about the same. These results convinced us that our spectrometer's behavior could be accurately described by our simulations, even in the presence of intense γ-rays and a thick target backing.

4. Experimental results

In order to search for the assumed X17 particle, both the energy-sum spectrum of the e^+e^- pairs measured by the telescopes, and their angular correlations, determined by the DSSD detectors, have been analyzed. For the real "signal" events we always required that the energy-sum for the e^+e^--pairs should be equal to the transition energy, which we want to investigate.

Since the counting rates in the detectors were low ($\approx$ 150 Hz in the scintillators and $\approx$ 25 Hz in the DSSD detectors) and the coincidence time window was sharp ($\approx$ 10 ns), the effect of random coincidences was negligible. In the following, we show only the real-coincidence gated spectra.

The down-scaled (x0.08) energy-sum spectrum of the e^+e^- pairs collected by all combinations of the telescope pairs in the 10 - 25 MeV energy range is shown by a dashed-line histogram in Fig. 4a) after subtracting the cosmic-ray background (CRB). This background was measured for two weeks before and after the experiments using the same gates and conditions as used for the in-beam data. It has been found that above E(sum)=25 MeV only the CRB contributes to the spectrum.

In order to reduce the External Pair Creation (EPC) background, we constructed a spectrum also from e^+e^- pairs, which were detected by telescope pairs with relative angles of 120°. The spectrum is shown in Fig. 4a) as a full-line histogram. The peak in the spectrum may come from the internal pairs created in the direct proton capture process or in the $0^+ \rightarrow 0^+$ E0 transition of ^{4}He and may also come from the e^+e^--decay of the X17 hypothetical particle. The background in the spectrum below E(sum)=17 MeV is created by external pairs induced by the γ-rays coming from the direct proton capture on the ^{3}H target.

The angular correlation spectra obtained for ^{4}He are indicated in Fig. 5(a) by dots, stars and full circles for E_p= 510, 610 and 900 keV, respectively. For better readability, the spectra are shifted by 1-1 orders of magnitude according to the labels.

The angular correlations of the e^+e^- pairs for the background region marked in Fig. 4 were also calculated, and compared to combinations of Monte Carlo simulations of different processes resulting in valid e^+e^- events in the spectrometer.

We found that the most significant background was provided by e^+e^- pairs created by γ-rays generated during direct proton capture on ^{3}H. For small correlation angles, this process can fully interpret the measured values. As a result of this, the normalization of the contribution of γ events was derived from the simulation's fit to the data in the 40° to 70° opening angle region.

Note that for the background regions of the sum-energy, the experimental and the corresponding simulated curves show a fairly good agreement over the entire angular range, thus validating the correctness of the simulations.

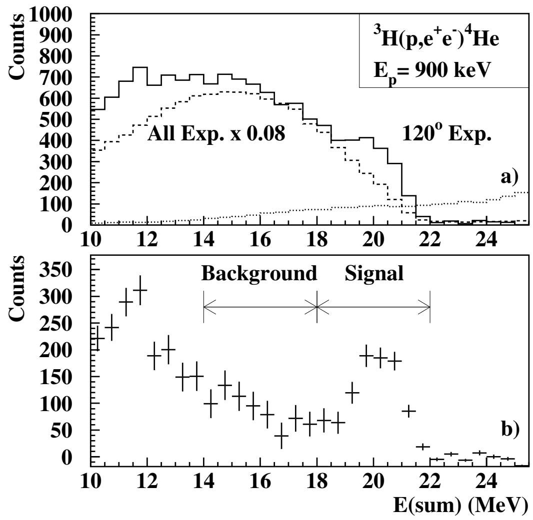

Figure 4. a): Experimental energy-sum spectra of the e^+e^- pairs derived, respectively, for "All" different detector combinations (dashed-line histogram with counts multiplied by 0.08) and for detectors at 120° relative angles (solid-line histogram). The cosmic-ray background contributions are subtracted from both spectra. The CRB spectrum corresponding to the "All" spectrum is plotted with dotted line. b): The markers with error bars show the difference of the solid-line and dashed-line distributions from Figure a).

Here we mention that in this case the usual method of background determination, i.e. performing the experiment without target material, cannot be applied because the main source of the background is the target material itself.

For further theoretical interpretation of the results shown in Fig. 5(a), the simulated angular correlations were subtracted from the experimental ones. The angular correlations (points with error bars) obtained after subtraction are shown in Fig. 5(b).

The corresponding proton beam energies are indicated in the figure. The anomaly previously observed and explained by the decay of the X17 particle appeared at each of the bombarding energies.

4.1. Fitting the angular correlations

In order to derive the exact value for the mass of the decaying particle from the present data, we carried out a fitting procedure for both the mass value and the amplitude of the observed peak.

The fit of the original experimental data was performed with RooFit [17] by describing the e^+e^- angular correlation with the following intensity function (INT):

$$INT = N_{EPC} * PDF(EPC) + N_{IPC} * PDF(IPC) + N_{Sig} * PDF(sig) \ , \tag{2}$$

where $PDF(X)$ stands for the MC-simulated probability density function and N_X is the fitted number of the events of the given process. $PDF(sig)$ was simulated by GEANT3 incorporating the relativistic two-body decay of a particle with a given mass. Therefore, $PDF(sig)$ was constructed as a 2-dimensional model as a function of the e^+e^- opening angle and the mass of

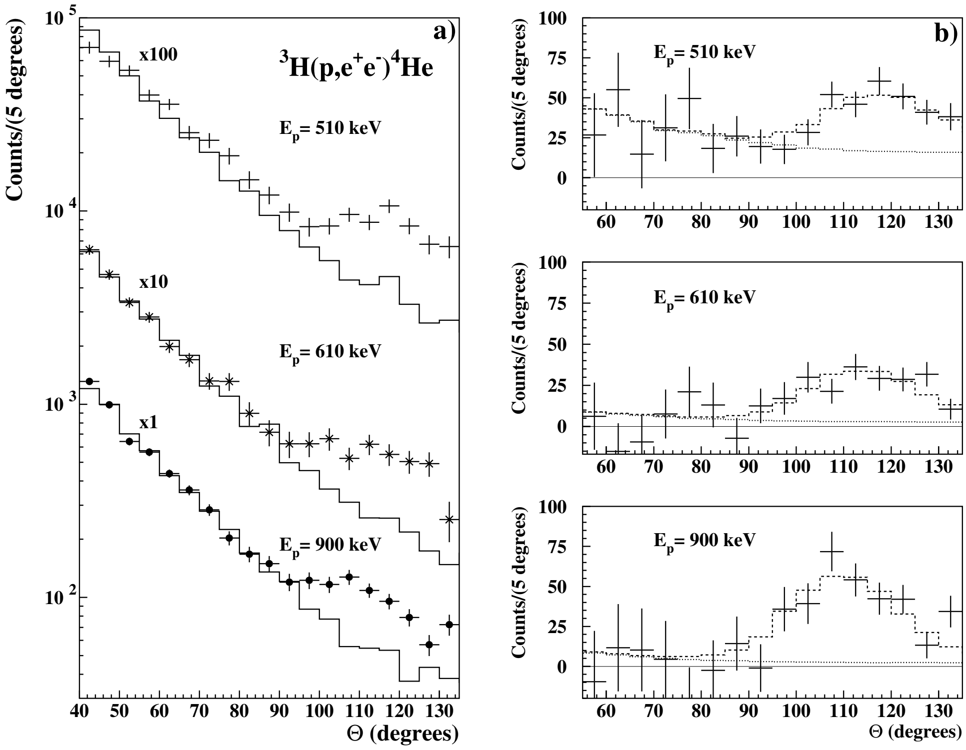

Figure 5. a): Angular correlations of the e^+e^- pairs for the "Signal" region (see Fig. 4). Symbols with error bars indicate experimental data measured in the ^{3}H(p,γ)^{4}He reaction at different proton beam energies, while solid-line histograms correspond to the respective data obtained in the simulations described in the text. b): Comparison of the experimental and the simulated angular correlations of the e^+e^- pairs. The best fitted sum (dashed line) as sum of the the simulated background (dotted line) and the simulated contribution of the hypothetical X17 boson is compared with the experimental signal values (dots with error bars)

the simulated particle. To construct the mass dependence, the PDF linearly interpolates the e^+e^- opening angle distributions simulated for discrete particle masses.

Using the intensity function described in Equation 2, we first performed a list of fits by fixing the simulated particle mass in the signal PDF to a certain value, and employing RooFit to estimate the best values for N_{Sig}, N_{EPC} and N_{IPC}. Allowing the particle mass to vary in the fit, the best fitted mass is calculated. We also made the fits by fixing the N_{EPC} value to the experimental data as described earlier.

The values obtained for the energy and branching ratio of the X17 boson and the IPC values, as a result of the average of the two fits described above, are summarized in Table 1, and the corresponding fits after subtraction of the EPC background are shown in Fig. 5(b).

4.2. Systematic uncertainties

The systematic uncertainties were estimated from the simulations. Taking into account the uncertainty of the target position along the beam line estimated to be ±2 mm, may cause an $\Delta m_X c^2 = \pm 0.06$ MeV uncertainty. The uncertainty of the position of the beam spot perpendicular to the beam axis was estimated to be ±2 mm in the worst case, which may cause a shift in the invariant mass of $\Delta m_X c^2 = \pm 0.15$ MeV. The total systematic error was

Table 1. Internal Pair Creation Coefficients (IPCC), X17 Boson branching ratios (B_x), masses of the X17 particle, and confidences derived from the fits.

E_p	IPCC	B_x	Mass	Confidence
(keV)	$\times10^{-4}$	$\times10^{-6}$	(MeV/c^2)	
510	2.5(3)	6.2(7)	17.01(12)	7.3σ
610	1.0(7)	4.1(6)	16.88(16)	6.6σ
900	1.1(11)	6.5(20)	16.68(30)	8.9σ
Averages		5.1(13)	16.94(12)	
^{8}Be values		6	16.70(35)	

conservatively estimated as: $\Delta m_{\rm X}c^2(\text{syst.}) = \pm0.21$ MeV.

4.3. Conclusions on X17

Table 1 shows the fitting parameters and the average of the parameters. As can be seen, consistent values were obtained for each fitting parameter. In the last row, our corresponding values measured in the case of ^{8}Be are also shown [3].

The obtained mass [13] agrees very well with that observed in the earlier ^{8}Be experiment, which is remarkable considering that the excesses in the observed angular correlation spectra appear at different correlation angles as one would indeed expect from the kinematics of the relativistic two-body decay. Therefore, our new observation enhances the possibility that the measured anomalies can be attributed to the same new particle X17.

As shown, the branching ratios of the X17 particle are identical within uncertainties, for the three beam energies proving that the X17 particle was most likely formed in direct proton capture, which has a dominant multipolarity of E1.

4.4. Preliminary results for the e^+e^- angular correlation from the $^{11}B(p,e^+e^-)^{12}C$ nuclear reaction.

The reaction was studied between $E_p = 1{,}5$ MeV and 2.9 MeV at 6 different bombarding energies. These energies covered the E_x= excitation energy region from 17.2 to 18.5 MeV, which included a wide resonance (E_x=17.23 MeV, $J^\pi=1^-$, Γ=1.05 MeV). The preliminary results are shown in Fig. 6.

According to the theoretical predictions, in the case of the smallest bombarding energy, the e^+e^- angular correlation could still be interpreted only by the internal pair creation process of the E1 multipolarity radiation since the excitation energy is very close to the threshold of X17 creation. In the case of higher energies it was already necessary to take into account the contribution of X17. In the case of different excitation energies, the location of the anomalous peak was constantly changing. At the same time the branching ratio compared to the E1 component of the radiation stayed constant. At the highest proton energy we were at off-resonance already, where we did not expect any anomaly.

With this, our experimental results confirmed the vectorial nature of the X17 particle and the protophobic interpretation of it, which could lead to the introduction of a fifth interaction and a better understanding of the properties of dark matter.

Our plans also include the study of the angular correlation of e^+e^- pairs generated by the decay of the giant dipole resonance (GDR) in the $^{11}B(p,e^+e^-)^{12}C$ nuclear reaction. In this case, the maximum of the anomaly related to the X17 is expected to be around 100°. Since GDR is observed in all nuclei, these results could trigger a systematic nuclear physics study of the X17 particle.

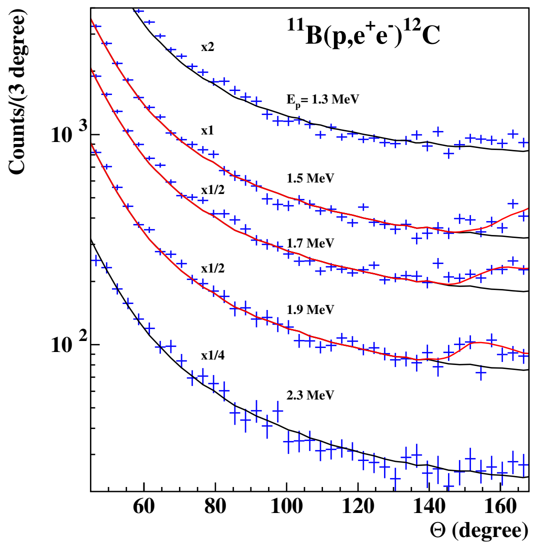

Figure 6. Angular correlations of the e^+e^- pairs obtained from the ^{11}B(p,γ)^{12}C reaction at different bombarding energies indicated in the figure. The simulated angular correlations for the X17 particle fitted to the data are also shown in red.

5. Acknowledgements

We wish to thank M. Viviani for providing us with their theoretical results. We wish to thank also Gy. Zilizi for providing us with the ^{3}H targets, Z. Pintye for the mechanical and J. Molnár for the electronic design of the experiment.

This work has been supported by the Hungarian NKFI Foundation No. K124810 and by the GINOP-2.3.3-15-2016-00034 and GINOP-2.3.3-15-2016-00034 grants.

References

[1] M. Pospelov, A. Ritz, and M.B. Voloshin, *Phys. Lett.* B **662** 53 (2008).
[2] T. Kitahara and Y. Yamamoto, *Phys. Rev.* D **95** 015008 (2017).
[3] A.J. Krasznahorkay et al., *Phys. Rev. Lett.* **116** 042501 (2016).
[4] M.E. Rose, Phys. Rev. **76**, (1949) 678. M.E. Rose, Phys. Rev. **78** 184 (1950).
[5] J. Feng et al., *Phys. Rev. Lett.* **117** 071803 (2016).
[6] J. Feng et al. *Phys. Rev.* D **95** 035017 (2017).
[7] Citations for Ref. [3]: https://inspirehep.net/search?ln=en&p=refersto%3Arecid%3A1358248&jrec=26&sf=earliestdate
[8] J. Gulyás et al. *Nucl. Instr. and Meth. in Phys. Res.* A **808**, 21 (2016).
[9] R. Brun, F. Bruyant, M. Maire, A.C. McPherson, P. Zanarini, Geant3 User's guide, Report number: CERN-DD-EE-84-01, (1987).
[10] K.E. Stiebing et al., J. Phys. G: Nucl. Part. Phys. **30** 165 (2004).
[11] U. Ellwanger and S. Moretti, J. High Energy Phys. **11** 39 (2016).
[12] Xilin Zhang, and Gerald A. Miller, Phys. Lett. **B 813** 136061 (2021).
[13] A. Krasznahorkay et al., Phys. Rev. C **104**, 044003 (2021).
[14] K.I. Hahn, C.R. Brune, and R.W. Kavanagh, Phys. Rev. C, 51 1624 (1995).
[15] D.R. Tilley, H.R. Weller, G.M. Hale, Nucl. Phys. **A541** 1 (1992).
[16] M. Viviani et al., Phys. Rev. C **105**, 014001 (2022).
[17] W. Verkerke and D. P. Kirkby, "The RooFit toolkit for data modeling," eConf C **0303241** (2003) MOLT007 [physics/0306116].